International Journal of Solids and Structures 41 (2004) 885–906

INTERNATIONAL JOURNAL OF SOLIDS and STRUCTURES

www.elsevier.com/locate/ijsolstr

Effective elastic properties of the particulate composite with transversely isotropic phases

V.I. Kushch [a,*], I. Sevostianov [b]

[a] Institute for Superhard Materials, National Academy of Sciences, 2 Avtozavodskaya Street, 04074 Kiev, Ukraine

[b] Department of Mechanical Engineering, New Mexico State University, P.O. Box 30001, Las Cruses, NM 88003, USA

Received 6 May 2003; received in revised form 2 September 2003

Abstract

The unit cell approach has been applied to study the effective elastic properties of a matrix type particulate composite with transversely isotropic phases. The microgeometry of composite is modeled by a periodic structure with a unit cell containing a certain number of arbitrarily placed and oriented spherical inclusions. The analytical, multipole expansion based method of solution has been developed reducing the complicated primary periodic boundary-value problem for a 3D multiple-connected domain to an ordinary set of linear algebraic equations and providing, thus, its high numerical efficiency. By analytical averaging the strain and stress fields the exact formulae for the effective stiffness tensor have been derived. The numerical results are given showing an efficiency and accuracy of the method and disclosing the way and extent to which the elastic properties mismatch, anisotropy degree and particle phase arrangement and orientation statistics influence macroscopic stiffness of composite.

Keywords: Composite materials; Spherical inclusions; Transversely isotropic materials; Linear elasticity; Multipole expansion; Effective moduli

1. Introduction

In the present work, the effective elastic properties of a particulate composite with transversely isotropic phases are evaluated using so-called "unit cell" approach. Its basic idea consists in modeling an actual microgeometry of composite by idealized periodic structure with a unit cell containing from one to several particles. Then, the homogenization boundary-value problem is to be stated and solved for the unit cell. Sometimes, this model is referred also as the "lattice" model reflecting the fact that the inclusions form a spatially periodic array. The model is advantageous in that it provides a natural way, through the periodic boundary conditions on the opposite cell facets, to take into account interactions among a whole infinite array of inhomogeneities. Also, the deterministic (although rather complicated) geometry of unit cell

* Corresponding author. Tel./fax: +380-444329544.
E-mail address: vkushch@bigmir.net (V.I. Kushch).

0020-7683/$ - see front matter
doi:10.1016/j.ijsolstr.2003.09.001

enables an accurate solution of the corresponding periodic boundary-value problems. These features make the unit cell approach to be appropriate for studying the high-filled strongly heterogeneous composites, where the structure and interactions between the particles should be taken into account to a maximum possible extent.

There is a number of papers where the unit cell approach has been applied to study the elastic properties of particulate composites with isotropic constituents. A periodic composite with the cubic lattice of rigid spherical particles was studied by Nunan and Keller (1984) by the method of singular integral equations. For a composite with elastic inclusions, an accurate solution has been obtained by Kushch (1987) and Sangani and Lu (1987) who used the multipole expansion method. For the composites with more general ellipsoidal shape of particles an approximate solution for the effective moduli has been obtained by Iwakuma and Nemat-Nasser (1983). Sangani and Mo (1997) and Kushch (1997b) considered more realistic structural model of composite with spheroidal inclusions and developed an accurate analytical, multipole expansion-based method of solution. Nemat-Nasser et al. (1993) and Kushch and Sangani (2000) applied the unit cell approach to evaluate elastic stiffness of the solids containing penny-shaped cracks.

Unlike the isotropic case, a few results can be found in literature relating the particulate composites with *anisotropic* phases. The most work done up to date in this area is based on the Green's function (point body force solution) for an infinite solid. Mura (1982) has derived the implicit Eshelby's type solution for a single inclusion in an anisotropic medium. Withers (1989) has obtained the Eshelby's tensor for an ellipsoidal inhomogeneity embedded in a transversely isotropic matrix. The exact variational bounds and self-consistent estimates for the scalar properties of anisotropic composites have been found in Willis (1977). Sevostianov et al. (2004) has derived expressions for components of the stiffness/compliance contribution tensors of a spheroidal inclusion embedded in a transversely isotropic matrix. They used the effective field method of Kanaun and Levin (1994) to calculate effective elastic properties of a composite with transversely isotropic phases. We also have to mention several papers addressing composite materials with transversely isotropic *piezoelectric* phases. Elastic properties can be obtained from these results as a particular case. So, in the method of conditional moments developed by Khoroshun et al. (1989), the one-point correlation of random stress and strain fields were retained in the solution. Various methods of averaging are discussed and detailed literature review is given by Sevostianov et al. (2001).

Noteworthy, in all the mentioned works the one-particle approximation based on the solution of the Eshelby problem is used. The structure parameters one can take into account in this model are shape of inclusions and volume content of disperse phase. Hence, one can expect it to work well for the composites with low and moderate volume content of disperse phase. The Willis (1975) paper is possibly the only work where the model with more that one inhomogeneity in an anisotropic elastic solid was considered. There, the problem for two interacting spherical voids was formulated in terms of integral equation for the transformation stress in equivalent homogeneous inclusion and, using the iterative perturbation technique, an explicit approximate solution has been obtained for polynomials up to second degree. The available by now applications of the unit cell model (e.g. Rodriguez-Ramos et al., 2001) are confined to the fiber reinforced composites. To the best knowledge of authors, this approach never been applied to the particulate composites with anisotropic constituents.

Recently, Kushch (2004) has extended the multipole expansion method on the transversely isotropic elasticity and obtained an accurate series solution for a solid containing a finite array of arbitrarily placed and oriented spherical inclusions. In the present paper, this method is further developed and combined with the unit cell model to evaluate the effective elastic properties of particulate composite with transversely isotropic phases. To expose a basic technique of the method, the simple periodic model is considered first. Then, an accurate solution for the generalized periodic structure is obtained. The finite exact expression of the effective elastic stiffness tensor is derived by analytical averaging of the strain and stress fields. The numerical results are presented and discussed in Section 6.

2. The problem statement

In the Cartesian coordinate system O_{xyz} with O_z axis aligned with the anisotropy axis of transversely isotropic elastic material, the generalized Hook's law $\boldsymbol{\sigma} = \mathbf{C} \cdot \cdot \boldsymbol{\varepsilon}$ has the form

$$\begin{aligned} \sigma_x &= C_{11}\varepsilon_x + C_{12}\varepsilon_y + C_{13}\varepsilon_z, \qquad & \tau_{xz} &= 2C_{44}\varepsilon_{xz}, \\ \sigma_y &= C_{12}\varepsilon_x + C_{11}\varepsilon_y + C_{13}\varepsilon_z, \qquad & \tau_{yz} &= 2C_{44}\varepsilon_{yz}, \\ \sigma_z &= C_{13}\varepsilon_x + C_{13}\varepsilon_y + C_{33}\varepsilon_z, \qquad & \tau_{xy} &= (C_{11} - C_{12})\varepsilon_{xy}. \end{aligned} \tag{1}$$

Here, two-indices notation $C_{ij} = C_{iijj}$ is accepted for components of the fourth rank stiffness tensor $\mathbf{C}$. The components of the stress tensor $\boldsymbol{\sigma}$ satisfy the elastic equilibrium equations $\nabla \cdot \boldsymbol{\sigma} = 0$ and the small strain tensor $\boldsymbol{\varepsilon}$ is related to the displacement vector $\mathbf{u}$ by $\boldsymbol{\varepsilon} = \frac{1}{2}[\nabla \mathbf{u} + (\nabla \mathbf{u})^{\mathrm{T}}]$.

We consider two-phase composite material consisting of a continuous phase (matrix) with embedded spherical inclusions of radius R. The matrix and inclusions are assumed to be elastic and transversely isotropic and perfectly bonded:

$$(\mathbf{u}^+ - \mathbf{u}^-)|_S = 0, \qquad (\mathbf{T}(\mathbf{u}^+) - \mathbf{T}(\mathbf{u}^-))|_S = 0, \tag{2}$$

where $\mathbf{T} = \boldsymbol{\sigma} \cdot \mathbf{n}$ the normal traction vector and $\mathbf{n}$ is the outer normal unit vector at the surface S. Here and below, all the parameters associated with the matrix and inclusion are denoted by the superscript "−" and "+", respectively: $\mathbf{C} = \mathbf{C}^-$ in the matrix and $\mathbf{C} = \mathbf{C}^+$ in the inclusions. We do not assume the anisotropy axes of the matrix and inclusion materials to be aligned and introduce the material-related Cartesian coordinate systems $O_{x^-y^-z^-}$ and $O_{x^+y^+z^+}$ with common origin in the center of inclusion. The coordinates of a point and the vector components in these coordinate bases are related by

$$x_i^+ = \Omega_{ij} x_j^-, \qquad u_i^+ = \Omega_{ij} u_j^-, \tag{3}$$

where $\boldsymbol{\Omega}$ is the rotation matrix: $\boldsymbol{\Omega}^{\mathrm{T}} = \boldsymbol{\Omega}^{-1}$ and $\det \boldsymbol{\Omega} = 1$.

We assign the macroscopic strain tensor

$$\mathbf{E} = \langle \boldsymbol{\varepsilon} \rangle = \frac{1}{V} \int\int_V \int \boldsymbol{\varepsilon} \, \mathrm{d}V \tag{4}$$

to be a governing parameter of the problem, V being a representative volume of composite. Alternatively, the loading parameter can be taken in the form of macroscopic stress tensor, $\mathbf{S} = \langle \boldsymbol{\sigma} \rangle = \frac{1}{V} \int\int\int_V \boldsymbol{\sigma} \, \mathrm{d}V$. We consider macroscopically homogeneous stress state of composite assuming both the $\mathbf{E}$ and $\mathbf{S}$ to be constant. Due to linearity of the problem, the relationship between these tensors can be written in the form

$$\langle \boldsymbol{\sigma} \rangle = \mathbf{C}^* \langle \boldsymbol{\varepsilon} \rangle, \tag{5}$$

where $\mathbf{C}^*$ is the macroscopic, or "effective", stiffness tensor of a composite. The main objective of this paper is to determine the tensor $\mathbf{C}^*$ of a particulate composite with transversely isotropic phases. It will be accomplished by solving a series of the model problems: namely, $\mathbf{C}^*_{ijkl} = \langle \sigma_{ij} \rangle$ provided that components of the macroscopic strain tensor are given by $\langle \varepsilon_{mn} \rangle = \delta_{mk}\delta_{nl}$, where δ_{ij} is the Kronecker's delta.

3. Unit cell model

3.1. Simple cubic lattice of inclusions

To expose the basic technique of the method, we consider first the simplest periodic model of particulate composite consisting of a continuous matrix with a periodic array of equal spherical inclusions of radius R

embedded. The centers of particles lie in the nodes of simple cubic (SC) lattice. Geometry of this model is defined either by the distance a between the neighbouring particles or, alternatively, by the volume content of dispersed phase $c = \frac{4}{3}\pi(R/a)^3$. To solve for this model accurately, we shall follow the approach developed by Kushch (1997b) and decompose the displacement vector $\mathbf{u}^-$ in the matrix domain into a sum of linear part $\mathbf{U}_0 = \mathbf{E}\cdot\mathbf{r}^-$ and periodic disturbance $\mathbf{U}_1$ produced by the inhomogeneities. It follows from (32) that $\mathbf{u}^- = \mathbf{U}_0 + \mathbf{U}_1$ comply the condition (4).

The disturbance displacement field $\mathbf{U}_1$ is a periodic function of spatial coordinates and, hence, can be expanded into a series over the triply periodic solutions $\widehat{\mathbf{F}}_{ts}^{(j)}$ of the equilibrium equations. Their explicit form is given by (A.11), where the functions F_t^s (A.7) are replaced by their periodic counterparts, $\widehat{F}_{ts}$ (B.1). The lattice nodes are the singularity points of these functions and, thus, $\widehat{\mathbf{F}}_{ts}^{(j)}$ can be thought as the periodic singular solution. Thus, we have

$$\mathbf{u}^- = \mathbf{E}\cdot\mathbf{r}^- + \sum_{j=1}^{3}\sum_{t=1}^{\infty}\sum_{|s|\leqslant t+1} A_{ts}^{(j)}\widehat{\mathbf{F}}_{ts}^{(j)}(\mathbf{r}^-), \tag{6}$$

where $A_{ts}^{(j)}$ are the unknown series expansion coefficients.

On the contrary, the displacement field $\mathbf{u}^+$ within an inclusion has no singularity and hence its series expansion contains the regular solutions $\mathbf{f}_{ts}^{(j)}$ only:

$$\mathbf{u}^+ = \sum_{j=1}^{3}\sum_{t=0}^{\infty}\sum_{|s|\leqslant t+1} D_{ts}^{(j)}\mathbf{f}_{ts}^{(j)}(\mathbf{r}^+). \tag{7}$$

Here, $D_{ts}^{(j)}$ as well as $A_{ts}^{(j)}$ in (6) are the unknown constants which are to be chosen so that to satisfy the interface boundary conditions (2). To obtain a resolving set of equations for the unknowns $A_{ts}^{(i)}$ and $D_{ts}^{(i)}$, we utilize the representation (A.12) of the functions $\mathbf{F}_{ts}^{(i)}$ and $\mathbf{f}_{ts}^{(i)}$ on the surface $r = R$, rewritten in the compact form as

$$\mathbf{F}_{ts}^{(i)}|_S = \sum_{j=1}^{3} UG_{ts}^{ji}\chi_t^{s_j}\mathbf{e}_j, \qquad \mathbf{f}_{ts}^{(i)}|_S = \sum_{j=1}^{3} UM_{ts}^{ji}\chi_t^{s_j}\mathbf{e}_j, \tag{8}$$

where

$$\mathbf{UG}_{ts} = \left\{UG_{ts}^{ij}\right\} = \begin{pmatrix} Q_t^{s-1}(\xi_{10}) & Q_t^{s-1}(\xi_{20}) & Q_t^{s-1}(\xi_{30}) \\ -Q_t^{s+1}(\xi_{10}) & -Q_t^{s+1}(\xi_{20}) & Q_t^{s+1}(\xi_{30}) \\ \frac{k_1}{\sqrt{v_1}}Q_t^s(\xi_{10}) & \frac{k_2}{\sqrt{v_2}}Q_t^s(\xi_{20}) & 0 \end{pmatrix},$$

$$\mathbf{UM}_{ts} = \left\{UM_{ts}^{ij}\right\} = \begin{pmatrix} P_t^{s-1}(\xi_{10}) & P_t^{s-1}(\xi_{20}) & P_t^{s-1}(\xi_{30}) \\ -P_t^{s+1}(\xi_{10}) & -P_t^{s+1}(\xi_{20}) & P_t^{s+1}(\xi_{30}) \\ \frac{k_1}{\sqrt{v_1}}P_t^s(\xi_{10}) & \frac{k_2}{\sqrt{v_2}}P_t^s(\xi_{20}) & 0 \end{pmatrix}$$

and $\mathbf{e}_i$ are the complex Cartesian vectors defined in Appendix A; $s_1 = s-1$, $s_2 = s+1$ and $s_3 = s$. Substituting (8) into (7) gives us

$$\mathbf{u}^+ = \sum_{i=1}^{3}\sum_{t=0}^{\infty}\sum_{|s|\leqslant t+1}\left[\sum_{\alpha=1}^{3} UM_{ts}^{i\alpha+}D_{ts}^{(\alpha)}\right]\chi_t^{s_i}(\theta^+,\varphi^+)\mathbf{e}_i^+. \tag{9}$$

To obtain the local expansion of $\mathbf{u}^-$ (6) in the form analogous to (9) we note that the regular part $\mathbf{U}_0$ can be written as a linear combination of the functions $\mathbf{f}_{1s}^{(j)}$, whose Cartesian components are the polynomials of first order. After some algebra, we get

$$\mathbf{E}\cdot\mathbf{r}^- = \sum_{j=1}^{3}\sum_{t=0}^{\infty}\sum_{|s|\leqslant t+1} e_{ts}^{(j)}\mathbf{f}_{ts}^{(j)}(\mathbf{r}^-), \tag{10}$$

where

$$\begin{aligned}
e_{10}^{(1)} &= \frac{d_1^- v_1^-}{k_1^- v_2^- - k_2^- v_1^-}[E_{33}v_2^- + k_2^-(E_{11}+E_{22})],\\
e_{11}^{(1)} &= -\overline{e_{1,-1}^{(1)}} = \frac{d_1^-\sqrt{v_1^-}}{k_1^-}(E_{13}-\mathrm{i}E_{23}),\\
e_{12}^{(1)} &= \overline{e_{1,-2}^{(1)}} = (E_{11}-E_{22}-2\mathrm{i}E_{12}),\\
e_{10}^{(2)} &= -\frac{v_2^- d_2^-}{k_1^- v_2^- - k_2^- v_1^-}[E_{33}v_1^- + k_1^-(E_{11}+E_{22})],\\
e_{11}^{(3)} &= \overline{e_{1,-1}^{(3)}} = \frac{\sqrt{v_3^-}d_3^-}{k_1^-}(1-k_1^-)(E_{13}-\mathrm{i}E_{23}),
\end{aligned} \tag{11}$$

all other coefficients $e_{ts}^{(i)}$ are equal to zero. For the definiteness sake, we assume here and below $v_1 \neq v_2$; in the case of equal roots v_1 and v_2 of Eq. (A.3), one has to use $\mathbf{f}_{ts}^{(2)}$ and $\mathbf{F}_{ts}^{(2)}$ in the form (A.16) rather than (A.11) in (6)–(10) and all the subsequent formulae.

Expansion of the periodic part $\mathbf{U}_1$ utilizes the formula

$$\widehat{\mathbf{F}}_{ts}^{(i)}(\mathbf{r},d_i) = \mathbf{F}_{ts}^{(i)}(\mathbf{r},d_i) + \sum_{k=0}^{\infty}\sum_{|l|\leqslant k+1}\hat{\eta}_{tk,s-l}(0,d_i)\mathbf{f}_{kl}^{(i)}(\mathbf{r},d_i) \tag{12}$$

following directly from the corresponding formula for scalar harmonics (B.10). Combining (6) with (12) and (8), we come to

$$\mathbf{u}^- = \sum_{j=1}^{3}\sum_{t=0}^{\infty}\sum_{|l|\leqslant t+1}\left[\sum_{\alpha=1}^{3} UG_{tl}^{j\alpha-}A_{tl}^{(\alpha)} + UM_{tl}^{j\alpha-}(a_{tl}^{(\alpha)}+e_{tl}^{(\alpha)})\right]\chi_t^{l_j}(\theta^-,\varphi^-)\mathbf{e}_j^-, \tag{13}$$

where

$$a_{ts}^{(j)} = \sum_{k=0}^{\infty}\sum_{|l|\leqslant k+1}\hat{\eta}_{kt,l-s}(0,d_j^-)A_{kl}^{(j)} \tag{14}$$

and $\hat{\eta}_{kt}^{(l-s)}$ are the triple infinite (lattice) sums given by (B.11) (Appendix B).

The local expansions of $\mathbf{u}^-$ (13) and $\mathbf{u}^+$ (9) are still written in the differently oriented coordinate bases. Therefore, before substituting them into (2), $\mathbf{u}^+$ has to be expressed in terms of the variables θ^-, φ^- and vectors $\mathbf{e}_j^-$. To this end, we apply the formula derived by Bateman and Erdelyi (1953):

$$\chi_t^s(\theta^+,\varphi^+) = \sum_{|l|\leqslant t}\frac{(t+l)!}{(t+s)!}S_{2t}^{t-s,t-l}(\mathbf{w})\chi_t^l(\theta^-,\varphi^-), \tag{15}$$

where S_{2t}^{sl} are the spherical harmonics in four-dimensional space and $\mathbf{w}$ is the vector of Euler's parameters related to the rotation matrix $\mathbf{\Omega}$ by

$$\mathbf{\Omega} = \begin{pmatrix} w_2^2-w_1^2-w_3^2+w_4^2 & 2(w_2w_3-w_1w_4) & 2(w_1w_2+w_3w_4)\\ 2(w_2w_3+w_1w_4) & w_3^2-w_1^2-w_2^2+w_4^2 & 2(w_1w_3-w_2w_4)\\ 2(w_1w_2-w_3w_4) & 2(w_1w_3-w_2w_4) & w_1^2-w_2^2-w_3^2+w_4^2 \end{pmatrix}. \tag{16}$$

Transformation of the vectors $\mathbf{e}_i$ uses the formula

$$\mathbf{e}_i^+ = \Omega_{ij}^* \mathbf{e}_j^-, \quad \text{where } \boldsymbol{\Omega}^* = \mathbf{D}^{-1}\boldsymbol{\Omega}\mathbf{D} \quad \text{and} \quad \mathbf{D} = \begin{pmatrix} 1 & 1 & 0 \\ -i & i & 0 \\ 0 & 0 & 1 \end{pmatrix}. \tag{17}$$

Applying (15) and (17) to (9) gives

$$\mathbf{u}^+ = \sum_{j=1}^{3} \sum_{t=0}^{\infty} \sum_{|l| \leqslant t+1} \left[\sum_{i=1}^{3} \Omega_{ij}^* \sum_{|s| \leqslant t+1} \frac{(t+l_j)!}{(t+s_i)!} S_{2t}^{t-s_i, t-l_j}(\mathbf{w}) \times \sum_{\alpha=1}^{3} UM_{ts}^{i\alpha+} D_{ts}^{(\alpha)} \right] \chi_t^{s_i}(\theta^-, \varphi^-) \mathbf{e}_i^-. \tag{18}$$

Now, we substitute $\mathbf{u}^-$ (13) and transformed expression of $\mathbf{u}^+$ (18) into the first of conditions (2) and exploit the orthogonality property of spherical harmonics χ_t^s on the surface S to decompose the vectorial functional equality $\mathbf{u}^+ = \mathbf{u}^-$ into a set of linear algebraic equations. In matrix notation, it can be written as

$$\mathbf{UG}_{tl}^- \cdot \mathbf{A}_{tl} + \mathbf{UM}_{tl}^- \cdot (\mathbf{a}_{tl} + \mathbf{e}_{tl}) = \sum_{|s| \leqslant t+1} \mathbf{UM}_{tsl}^* \cdot \mathbf{D}_{ts}, \quad t = 0, 1, 2, \ldots, \quad |l| \leqslant t+1, \tag{19}$$

where

$$\mathbf{UM}_{tsl}^* = \mathbf{W}_{tsl} \mathbf{UM}_{ts}^+, \qquad W_{tsl}^{ji} = \Omega_{ij}^* \frac{(t+l_j)!}{(t+s_i)!} S_{2t}^{t-s_i, t-l_j}(\mathbf{w}), \tag{20}$$

$$\mathbf{A}_{tl} = (A_{tl}^{(1)}, A_{tl}^{(2)}, A_{tl}^{(3)})^{\mathrm{T}} \quad \text{and} \quad \mathbf{a}_{tl} = (a_{tl}^{(1)}, a_{tl}^{(2)}, a_{tl}^{(3)})^{\mathrm{T}},$$

the vectors $\mathbf{D}_{tl}$ and $\mathbf{e}_{tl}$ are of the same structure.

Obtaining the second set of equations follows the same way with only difference that, instead of (A.12), the representation (A.13) of the normal traction vectors $\mathbf{T_n}(\mathbf{f}_{ts}^{(j)})$ and $\mathbf{T_n}(\mathbf{f}_{ts}^{(j)})$ on the surface $r = R$ is to be utilized. After transformations, we obtain

$$\mathbf{TG}_{tl}^- \cdot \mathbf{A}_{tl} + \mathbf{TM}_{tl}^- \cdot (\mathbf{a}_{tl} + \mathbf{e}_{tl}) = \sum_{|s| \leqslant t+1} \mathbf{TM}_{tsl}^* \cdot \mathbf{D}_{ts}, \tag{21}$$

where $\mathbf{TM}_{tsl}^* = \mathbf{W}_{tsl} \mathbf{TM}_{ts}^+$. Form of the matrices $\mathbf{TG}_{tl}$ and $\mathbf{TM}_{tl}$ is clear form (A.13). Eqs. (19) and (21) together form a complete set of linear equations from where $A_{ts}^{(i)}$ and $D_{ts}^{(i)}$ can be determined. An attempt to solve this linear system discovers, however that its determinant is equal to zero. The reason is that, for a given t, some of the functions $\mathbf{f}_{ts}^{(i)}$ at $|s| \geqslant t$ are linearly dependent: e.g., $\mathbf{f}_{t,t+1}^{(1)} \sim \mathbf{f}_{t,t+1}^{(2)}$ and $\mathbf{f}_{t,t+1}^{(2)} \sim \mathbf{f}_{t,t+1}^{(3)}$. Really, we have $3(2t+3)$ vectorial solutions of order t introduced whereas the number of independent functions is equal to $3(2t+1)$ (remind, the Cartesian components of $\mathbf{f}_{ts}^{(i)}$ are the polynomials of order t (A.11) and $f_t^s \equiv 0$ for $|s| > t$). Due to the same reason, not all the $e_{1s}^{(j)}$ are represented in (11). Adding six additional constraints $D_{t,\pm t}^{(2)} = 0$, $D_{t,\pm(t+1)}^{(2)} = 0$ and $D_{t,\pm(t+1)}^{(3)} = 0$ to (19) and (21) gives, finally, a well-posed set of linear equations possessing an unique solution.

3.2. Generalized periodic structure model

Let us consider now a composite of periodic structure with a unit cell of cubic form containing N non-touching equal-sized spherical particles with the centers located in the points O_q, $q = 1, 2, \ldots, N$. We introduce the local material-related coordinate systems $O_{x_q^+ y_q^+ z_q^+}$ which origin and orientation with respect to the global Cartesian coordinate system $O_{x^- y^- z^-}$ is defined by the vector $\mathbf{R}_q$ and the rotation matrix $\boldsymbol{\Omega}_q$. The matrix-inclusion interface conditions, consistent with (2), are

$$(\mathbf{u}_q^+ - \mathbf{u}^-)|_{S_q} = 0, \quad (\mathbf{T_n}(\mathbf{u}_q^+) - \mathbf{T_n}(\mathbf{u}^-))|_{S_q} = 0, \quad q = 1, 2, \ldots, N. \tag{22}$$

In (22), $\mathbf{u}_q^+$ is the displacement vector in the volume of qth inclusion which, by analogy with (7) can be written as

$$\mathbf{u}_q^+ = \sum_{j=1}^{3}\sum_{t=0}^{\infty}\sum_{|s|\leqslant t+1} D_{ts}^{(q)(j)}\mathbf{f}_{ts}^{(j)}(\mathbf{r}_q^+). \tag{23}$$

To construct solution for a multiply connected matrix domain, we shall follow the procedure described by Kushch (1997b). According to the superposition principle, the displacement vector $\mathbf{u}^-$ can be written as a sum of linear far field and the disturbance fields induced by each separate inclusion:

$$\mathbf{u}^- = \mathbf{E}\cdot\mathbf{r}^- + \sum_{p=1}^{N}\mathbf{U}_p(\mathbf{r}_p), \qquad \mathbf{r}_p = \mathbf{r}^- - \mathbf{R}_p. \tag{24}$$

By analogy with (6), each singular term $\mathbf{U}_p$ allows series expansion of the form

$$\mathbf{U}_p(\mathbf{r}_p) = \sum_{j=1}^{3}\sum_{t=0}^{\infty}\sum_{|s|\leqslant t+1} A_{ts}^{(p)(j)}\widehat{\mathbf{F}}_{ts}^{(j)}(\mathbf{r}_p^-), \tag{25}$$

where $A_{ts}^{(p)(j)}$ as well as $D_{ts}^{(q)(j)}$ in (23) are the series expansion coefficients to be found from the boundary conditions (22).

Note that the separate terms of the sum in (25) are written in the different coordinate systems. To enable application the procedure described in the previous section, we need first to express $\mathbf{u}^-$ in the variables of the local, say qth, coordinate system. Such a transform for $p \neq q$ is based on using the re-expansion formulae for the singular vectorial solutions $\mathbf{F}_{ts}^{(j)}$ due to translation of the coordinate system origin:

$$\widehat{\mathbf{F}}_{ts}^{(j)}(\mathbf{r}_p^-) = \sum_{k=0}^{\infty}\sum_{|l|\leqslant k+1}\hat{\eta}_{tk,s-l}(\mathbf{R}_{pq}, d_j^-)\mathbf{f}_{kl}^{(j)}(\mathbf{r}_q^-), \quad t = 0,1,2,\ldots, \quad |s|\leqslant t+1, \tag{26}$$

following directly from the corresponding result for the scalar harmonic functions F_t^s (B.2). We apply (26) to all the sum terms in (25) but that one with $p = q$ which requires (12) to be applied. After some algebra, we find

$$\mathbf{u}^-(\mathbf{r}_q^-) = \sum_{j=1}^{3}\sum_{t=0}^{\infty}\sum_{|s|\leqslant t+1}\left[A_{ts}^{(q)(j)}\mathbf{F}_{ts}^{(j)}(\mathbf{r}_q^-) + (a_{ts}^{(q)(j)} + e_{ts}^{(q)(j)})\mathbf{f}_{ts}^{(j)}(\mathbf{r}_q^-)\right], \tag{27}$$

where

$$a_{ts}^{(q)(j)} = \sum_{k=0}^{\infty}\sum_{|l|\leqslant k+1}\sum_{p=1}^{N}\hat{\eta}_{kt,l-s}(\mathbf{R}_{pq}, d_j^-)A_{kl}^{(p)(j)} \tag{28}$$

and $e_{ts}^{(q)(j)}$ are the expansion coefficients of the linear part of (24) given by the formula (10).

After the local expansion of $\mathbf{u}^-$ in the vicinity of the point O_q is found, the remaining part of solving procedure follows the way described in the Section 3.1. The resolving set of linear algebraic equations is

$$\begin{aligned}
&\mathbf{UG}_{tl}^{(q)-}\cdot\mathbf{A}_{tl}^{(q)} + \mathbf{UM}_{tl}^{(q)-}\cdot(\mathbf{a}_{tl}^{(q)} + \mathbf{e}_{tl}^{(q)}) = \sum_{|s|\leqslant t+1}\mathbf{M}_{tsl}^{(q)*}\cdot\mathbf{D}_{ts}^{(q)},\\
&\mathbf{TG}_{tl}^{(q)-}\cdot\mathbf{A}_{tl}^{(q)} + \mathbf{TM}_{tl}^{(q)-}\cdot(\mathbf{a}_{tl}^{(q)} + \mathbf{e}_{tl}^{(q)}) = \sum_{|s|\leqslant t+1}\mathbf{TM}_{tsl}^{(q)*}\cdot\mathbf{D}_{ts}^{(q)},\\
&\quad q = 1,2,\ldots,N, \;\; t = 0,1,2,\ldots, \;\; |l|\leqslant t+1,
\end{aligned} \tag{29}$$

where $\mathbf{a}_{tl}^{(q)} = \left(a_{ts}^{(q)(j)}, a_{ts}^{(q)(j)}, a_{ts}^{(q)(j)}\right)^{\mathrm{T}}$ and $a_{ts}^{(q)(j)}$ are given by (28). Its approximate solution can be obtained by the truncation method, when the unknowns and equations with $t \leqslant t_{\max}$ only are retained in the (29). The solution is convergent for $t_{\max} \to \infty$ provided that the non-touching conditions $\|\mathbf{R}_{pq}\| > 2R$ are satisfied for each pair of inclusions. Thus, we can solve (29) for $\mathbf{A}_{tl}^{(q)}$ and $\mathbf{D}_{ts}^{(q)}$ with any desirable accuracy by taking $t_{\max}$ sufficiently large. It is seen form the Table 1 in the Section 5 that the convergence rate is sufficiently high for a whole range of the problem parameters excluding only the nearly touching rigid inclusions. An asymptotic analysis of this extreme case, however, is beyond the scope of this paper.

4. Effective stiffness tensor

The macroscopic, or effective, elastic stiffness tensor is defined by Eq. (5) where, due to periodicity of structure, the unit cell can be taken as a representative volume element of periodic composite. For such a composite, integration of the strain and stress fields corresponding to the displacement vector (23), (24) can be carried out analytically. As it was mentioned already, the components of the effective stiffness tensor can be found as $\mathbf{C}_{ijkl}^* = \langle \sigma_{ij} \rangle$, where the stress $\boldsymbol{\sigma}$ is calculated for $\langle \varepsilon_{kl} \rangle = 1$, $\langle \varepsilon_{k'l'} \rangle = 0 (k \neq k',\ l \neq l')$. First, we apply the Gauss' theorem to calculate the average strain:

$$V\langle \varepsilon_{ij} \rangle = \int\!\!\int_{V^-}\!\!\int \varepsilon_{ij}^- \,\mathrm{d}V + \sum_{q=1}^{N} \int\!\!\int_{V_q^+}\!\!\int \varepsilon_{ij}^+ \,\mathrm{d}V$$
$$= \frac{1}{2}\int\!\!\int_{\Sigma} (u_i^- n_j + u_j^- n_i)\,\mathrm{d}S + \frac{1}{2}\sum_{q=1}^{N}\int\!\!\int_{S_q} \left[\left(u_i^{(q)+} - u_i^-\right)n_j + \left(u_j^{(q)+} - u_j^-\right)n_i\right]\mathrm{d}S, \tag{30}$$

where V_q is domain occupied by qth inclusion, $V = V^- + \sum_{q=1}^{N} V_q^+$ and Σ is the unit cell boundary. Taking the first of interface conditions (2) and periodicity of solution (24) into account, we get easily

$$\langle \varepsilon_{ij} \rangle = \frac{1}{2V}\int\!\!\int_{\Sigma} (u_i^- n_j + u_j^- n_i)\,\mathrm{d}S = E_{ij}, \tag{31}$$

i.e. $\mathbf{E}$ has a meaning of the macroscopic strain tensor, in accordance with (4). Thus,

$$\mathbf{C}_{ijkl}^* = \langle \sigma_{ij} \rangle|_{E_{mn} = \delta_{mk}\delta_{nl}}. \tag{32}$$

To compute the average stress, we make use of the identity $\sigma_{ij} = \frac{\partial}{\partial x_k}(x_j \sigma_{ik})$ and the Gauss' theorem to obtain

$$V\langle \sigma_{ij} \rangle = \int\!\!\int_{V^-}\!\!\int \sigma_{ij}\,\mathrm{d}V + \sum_{q=1}^{N}\int\!\!\int_{V_q^+}\!\!\int \sigma_{ij}\,\mathrm{d}V = \int\!\!\int_{\Sigma} \sigma_{ik}^- n_k x_j\,\mathrm{d}S + \sum_{q=1}^{N}\int\!\!\int_{S_q}\left(\sigma_{ik}^{(q)+} n_k - \sigma_{ik}^- n_k\right) x_j\,\mathrm{d}S. \tag{33}$$

Table 1
Convergence rate of the effective stiffness C_{33}^* of composite with SC lattice of inclusions with $t_{\max}$ increased, $A = 5$

$t_{\max}$	$c = 0.1$		$c = 0.3$		$c = 0.5$	
	$\lambda = 0$	$\lambda = \infty$	$\lambda = 0$	$\lambda = \infty$	$\lambda = 0$	$\lambda = \infty$
1	8.274	12.41	5.664	19.60	3.614	32.84
3	8.257	12.42	5.534	20.39	3.307	43.71
5	8.257	12.43	5.533	20.48	3.292	49.21
7	8.257	12.43	5.533	20.49	3.289	52.11
9	8.257	12.43	5.533	20.49	3.287	53.47
11	8.257	12.43	5.533	20.49	3.286	54.16
13	8.257	12.43	5.533	20.49	3.285	54.48
15	8.257	12.43	5.533	20.49	3.285	54.57

According to (22), the traction vector $\mathbf{T} = \boldsymbol{\sigma} \cdot \mathbf{n}$ is continuous through the spherical interface S_q and, thus,

$$V\langle\sigma_{ij}\rangle = \iint_{\Sigma} T_i^- x_j \, \mathrm{d}S. \tag{34}$$

It follows from the Betti's reciprocal theorem that the equality

$$\left(\iint_{\Sigma} - \sum_{q=1}^{N} \iint_{S_q}\right)(T_k^- u_k' - T_k' u_k^-)\,\mathrm{d}S = 0, \tag{35}$$

where $\mathbf{T}' = \mathbf{T}(\mathbf{u}')$, is valid for any displacement vector $\mathbf{u}'$ satisfying the governing equations. We take it in the form $u_k' = \delta_{ik}x_j$; it is straightforward to show that in this case

$$\iint_{\Sigma} T_k^- u_k' \,\mathrm{d}S = \iint_{\Sigma} \sigma_{il}^- n_l x_j \,\mathrm{d}\Sigma = V\langle\sigma_{ij}\rangle. \tag{36}$$

On the other hand,

$$T_k' u_k^- = \sigma_{kl}' n_l u_k^- = \tfrac{1}{2} C_{mnkl}^- (\delta_{mi}\delta_{nj} + \delta_{mj}\delta_{ni}) n_l u_k^-, \tag{37}$$

comparison with (31) gives us

$$\frac{1}{V}\iint_{\Sigma} T_k' u_k^- \,\mathrm{d}\Sigma = C_{ij\alpha\alpha}^- \langle\varepsilon_{\alpha\alpha}\rangle\delta_{ij} + C_{ijij}^-\langle\varepsilon_{ij}\rangle(1-\delta_{ij}) \tag{38}$$

and, thus,

$$\langle\sigma_{ij}\rangle = C_{ij\alpha\alpha}^- \langle\varepsilon_{\alpha\alpha}\rangle\delta_{ij} + C_{ijij}^-\langle\varepsilon_{ij}\rangle(1-\delta_{ij}) + \frac{1}{V}\sum_{q=1}^{N}\iint_{S_q}(T_k^- u_k' - T_k' u_k^-)\,\mathrm{d}S. \tag{39}$$

The formula (39) is valid for an arbitrary orientation of inclusions and a general anisotropy type of phase materials. To compute average stress from (39), one needs to integrate the matrix fields only; with the local series expansions (13) and (27) taken into account, this task is rather trivial. Moreover, it follows from the Betti's theorem that for all the regular solutions $\mathbf{f}_{ts}^{(j)}$ these integrals are equal to zero. Among the singular solutions $\mathbf{F}_{ts}^{(j)}$, only those with $t = 1$ contribute $\langle\sigma_{ij}\rangle$: after some algebra, we get the *exact* explicit formulae:

$$\begin{aligned}
\langle\sigma_{11}\rangle &= C_{1k}^-\langle\varepsilon_{kk}\rangle - C_{11}^-\left(\sqrt{\nu_1^-}\tilde{A}_{10}^{(1)} + \sqrt{\nu_2^-}\tilde{A}_{10}^{(2)}\right) + \frac{C_{44}^-}{2}\frac{(1+k_j^-)}{\sqrt{\nu_j^-}}\mathrm{Re}\tilde{A}_{12}^{(j)},\\
\langle\sigma_{22}\rangle &= C_{2k}^-\langle\varepsilon_{kk}\rangle - C_{11}^-\left(\sqrt{\nu_1^-}\tilde{A}_{10}^{(1)} + \sqrt{\nu_2^-}\tilde{A}_{10}^{(2)}\right) - \frac{C_{44}^-}{2}\frac{(1+k_j^-)}{\sqrt{\nu_j^-}}\mathrm{Re}\tilde{A}_{12}^{(j)},\\
\langle\sigma_{33}\rangle &= C_{3k}^-\langle\varepsilon_{kk}\rangle - C_{33}^-\left(\frac{k_1^-}{\sqrt{\nu_1^-}}\tilde{A}_{10}^{(1)} + \frac{k_2^-}{\sqrt{\nu_2^-}}\tilde{A}_{10}^{(2)}\right),\\
\langle\sigma_{12}\rangle &= C_{66}^-\langle\varepsilon_{12}\rangle + \frac{C_{44}^-}{2}\frac{(1+k_j^-)}{\sqrt{\nu_j^-}}\mathrm{Im}\tilde{A}_{12}^{(j)},\\
\langle\sigma_{13}\rangle - i\langle\sigma_{23}\rangle &= C_{44}^-(\langle\varepsilon_{13}\rangle - i\langle\varepsilon_{23}\rangle) + \frac{C_{44}^-}{2}[(1+2k_1^-)\tilde{A}_{11}^{(1)} + (1+2k_2^-)\tilde{A}_{11}^{(2)} - \tilde{A}_{11}^{(3)}],
\end{aligned} \tag{40}$$

where $\tilde{A}_{1s}^{(j)} = (d^-)^2 \frac{c}{N}\sum_{q=1}^{N} A_{1s}^{(q)(j)}$.

5. Numerical results

In this section, we present several numerical examples demonstrating numerical efficiency and accuracy of the method developed and showing, at the same time, how the selected microstructure parameters influence the macroscopic elastic stiffness of a composite. Noteworthy, numerical algorithm of the method is rather simple and consists in computing the triple sums (B.11) which enter the matrix elements of the infinite algebraic system (39) and then solving the truncated linear system by some standard method. The typical number of unknowns retained in the resolving set of equations varies from tens to a several hundreds depending on complexity of the problem being considered. This is a very moderate number in comparison with the tens and hundreds of thousand equations in the 3D finite element analysis of similar problems which proves the above algorithm to be highly efficient form the computational standpoint.

With the number of inclusions inside the unit cell increased the computational effort of triple sums (B.11) evaluation grows as N^2 and, for N small, is the most time-consuming part of algorithm. However, for $N \gtrsim 10$, the proper choice of linear solver becomes important and, when the dimension of truncated system exceeds 10^3, the iterative algorithms rather than the direct $O(N^3)$ methods should be applied. The recent version of generalized minimum residual (GMRES) iterative solver by Fraysse et al. (1998) was found to be quite appropriate for this purpose. With using the iterative solving procedure, the total computational time scales as N^2 which enables carrying out the numerical simulations up to $N = 30$–40 on a regular PC. For a larger number of inclusions, an additional effort should be applied to provide fast and efficient numerical realization of the method. One straightforward way to do this is to incorporate the above solution into a general scheme of the $O(N)$ algorithm by Sangani and Mo (1995).

The problem considered has a number of parameters: they are five components of the matrix $\mathbf{C}^-$, five components of the matrix $\mathbf{C}^+$, three components of the position vector $\mathbf{R}_q$ and three components of the rotation matrix $\mathbf{\Omega}_q$ for each of N particles and six components of the macroscopic strain tensor, $\mathbf{E}$. An exhaustive parametric study of the problem is not a subject of the paper. Although no restrictions but the particle-to-particle non-touching condition were imposed on the structure, phase properties and loading type, in the subsequent numerical study we shall keep most of the parameters fixed and present the numerical data giving a general idea how spatial arrangement and orientation of the particles and anisotropy degree of phase materials affect the effective elastic stiffness of composite. Three particle arrangement types considered in our numerical study are:

(a) simple cubic (SC) structure, $N = 1$;
(b) body-centered cubic (BCC) structure, which can be thought as a particular case of a generalized periodic model with $N = 2$ and $\mathbf{R}_{12} = (a/2, a/2, a/2)$;
(c) quasi-random (QR) structure, $N = 16$.

In all above cases, $c = \frac{4}{3}\pi N(R/a)^3$, where a is the lattice period.

To minimize number of the independent elastic constants, we put $\nu_{12}^+ = \nu_{12}^- = 0.25$, $\nu_{13}^+ = \nu_{13}^- = 0.25$, $G_{13}^- = 1$ and $E_1^- = 2.0$. Here and below E_i, G_{ij} and ν_{ij} are the Young's moduli, the shear moduli and the Poisson's ratios, respectively, related to C_{ij} by

$$G_{12} = C_{66} = (C_{11} - C_{12})/2, \qquad G_{23} = G_{13} = C_{44},$$

$$E_1 = E_2 = 2\left(\frac{1}{C_{11} - C_{12}} + \frac{C_{33}}{\Delta}\right)^{-1}, \quad E_3 = \frac{\Delta}{(C_{11} + C_{12})},$$

$$\nu_{13} = \nu_{23} = C_{13}/(C_{11} + C_{12}), \quad \nu_{12} = \frac{E_1}{2}\left(\frac{1}{C_{11} - C_{12}} - \frac{C_{33}}{\Delta}\right),$$

where $\Delta = (C_{11} + C_{12})C_{33} - 2(C_{13})^2$ and only five of these constants are independent. Two variable material-related parameters are the matrix anisotropy degree $A = E_3^-/E_1^-$ and the inclusion-to-matrix stiffness ratio, λ. Thus, we have $E_3^- = AE_1^-$, $G_{13}^+ = \lambda G_{13}^-$, $E_1^+ = \lambda E_1^-$ and $E_3^+ = \lambda E_3^-$. Two extreme cases we focus our attention on are $\lambda = 0$ and $\lambda = \infty$, corresponding to the cavities and rigid particles. For the elastic inclusion $E_3^+/E_1^+ = A$; i.e., we assume the inclusion's anisotropy degree to be equal to that of the matrix material.

Remind that although the expressions for effective elastic moduli (32), (40) are finite and exact, the complete solution is given by the infinite series (23)–(25). For computations, we retain in theoretical solution a finite number of harmonics with $t \leqslant t_{\max}$ only and, to estimate accuracy of the numerical results obtained, one needs to learn about the convergence of truncated solution with $t_{\max}$ increased. The data presented in Table 1 show that, up to $c = 0.3$ at least, value $t_{\max} = 5$ is sufficient to provide four-digit accuracy. The convergence rate decreases significantly only in the extreme case of nearly touching rigid inclusions. However, even for $c = 0.5$, when the minimal distance between the surfaces of neighbouring inclusions is as small as 1% of their radii, the value $t_{\max} = 15$ provides three-digit accuracy of the effective moduli calculated. As it seen from the table, for a porous material ($\lambda = 0$) solution converges much more rapidly: for a composite with elastic inclusions of finite stiffness, we can expect intermediate convergence rate. Therefore, all the subsequent computations for composites of SC and BCC symmetry were performed with $t_{\max} = 15$. However, for a composite with QR-array of inclusions the value $t_{\max} = 7$ was adopted in order to reduce the computational effort. This choice was motivated by the fact that variation of the computed values from one quasi-random structure realization to another exceeds greatly possible improvement in accuracy of solution by taking into account the higher harmonics.

In Table 2, the effective elastic properties of composite of SC structure are given as a function of volume content of disperse phase. For $c = 0$, they are the equal to those of the matrix material: $C_{11}^* = 2.179$; $C_{12}^* = 0.579$; $C_{13}^* = 0.690$; $C_{33}^* = 10.344$ and $C_{44}^* = 1.0$. Here and below, we put the anisotropy degree $A = 5$. Analogous data for the composite of BCC structure are given in Table 3. It is clearly seen from these tables that the arrangement type affects the macroscopic properties of high-filled composite dramatically: for $c = 0.5$, C_{33}^* of composite with SC lattice of rigid particles more than two times exceeds C_{33}^* of composite of BCC structure. So wide difference is quite predictable because for a composite with rigid inclusions $C_{ij}^* \to \infty$ as $c \to c_{\max}$, where $c_{\max}$ is a volume content of dense packing of particles, equal to 0.52 for SC and 0.68 for BCC structure. Value $c = 0.5$ is close to $c_{\max}$ for SC array, resulting in much higher effective elastic moduli as compared with BCC lattice. For a composite with weak inclusions or porous material, this effect is less prominent because $\mathbf{C}^*$ remains finite even for $c = c_{\max}$.

Note that although only five components of effective stiffness tensor are shown in Tables 2 and 3, the periodic composite is not transversely isotropic on macro level even in the case of aligned anisotropy axes of the matrix and inclusions. In the model considered, one of the lattice basis vectors is aligned with the anisotropy axis of matrix material. Hence, one can expect the composite to be macroscopically orthotropic and an additional anisotropy degree induced by the periodicity of microstructure can be estimated as the ratio $(C_{11}^* - C_{12}^*)/2C_{66}^*$, equal to 1 for a transversely isotropic material. It seen from Table 4 that anisotropy is much stronger when the inclusions are arranged in the simple cubic array. On the other hand, the cavities

Table 2
Effective elastic properties of composite with SC lattice of cavities or rigid inclusions

c	C_{11}^*		C_{12}^*		C_{13}^*		C_{33}^*		C_{44}^*	
	$\lambda = 0$	$\lambda = \infty$	$\lambda = 0$	$\lambda = \infty$	$\lambda = 0$	$\lambda = \infty$	$\lambda = 0$	$\lambda = \infty$	$\lambda = 0$	$\lambda = \infty$
0.1	1.810	2.716	0.464	0.685	0.552	0.827	8.257	12.43	0.811	1.213
0.2	1.508	3.464	0.366	0.786	0.428	0.957	6.785	15.60	0.638	1.458
0.3	1.243	4.552	0.282	0.874	0.322	1.078	5.533	20.48	0.488	1.783
0.4	0.996	6.375	0.208	0.942	0.232	1.185	4.400	29.03	0.359	2.296
0.5	0.749	11.73	0.140	0.990	0.152	1.267	3.286	54.57	0.243	3.694

Table 3
Effective elastic properties of composite with BCC lattice of cavities or rigid inclusions

c	C_{11}^*		C_{12}^*		C_{13}^*		C_{33}^*		C_{44}^*	
	$\lambda=0$	$\lambda=\infty$	$\lambda=0$	$\lambda=\infty$	$\lambda=0$	$\lambda=\infty$	$\lambda=0$	$\lambda=\infty$	$\lambda=0$	$\lambda=\infty$
0.1	1.791	2.676	0.471	0.703	0.569	0.848	7.955	12.18	0.826	1.236
0.2	1.459	3.287	0.385	0.866	0.471	1.045	6.159	14.52	0.675	1.538
0.3	1.174	4.069	0.313	1.078	0.394	1.301	4.652	17.45	0.542	1.970
0.4	0.926	5.134	0.251	1.369	0.327	1.648	3.406	21.25	0.422	2.637
0.5	0.710	6.731	0.194	1.807	0.261	2.164	2.422	26.66	0.311	3.763
0.6	0.518	9.732	0.140	2.666	0.190	3.173	1.666	36.32	0.209	6.099

Table 4
Effective anisotropy degree $(C_{11}^* - C_{12}^*)/2C_{66}^*$ induced by the structure

c	SC structure		BCC structure	
	$\lambda=0$	$\lambda=\infty$	$\lambda=0$	$\lambda=\infty$
0.1	1.032	1.042	0.992	0.989
0.2	1.109	1.145	0.975	0.964
0.3	1.218	1.297	0.958	0.928
0.4	1.359	1.503	0.949	0.882
0.5	1.572	1.858	0.959	0.826

as well as the rigid particles can be thought as extreme case of isotropic inclusions: adding them to anisotropic matrix must change an effective anisotropy measured as a ratio of the effective Young's moduli, E_3^*/E_1^*. The relevant data given in Table 5 show that, with c growing, an anisotropy is decreasing to a bigger extent in the case of BCC packing of inclusions.

Now, we consider a periodic composite containing $N = 16$ particles randomly placed inside the unit cell. We call this structure as quasi-random (QR): it was shown elsewhere (e.g. Sangani and Lu, 1987), that the radial distribution function of such a structure is close to that predicted by the Percus–Yevick's equation for a perfectly disordered particulate composite. One can expect, therefore, the properties of our model to be close to the properties of composite with random microstructure. To generate the model, the molecular dynamics simulation algorithm similar to that described by Sangani and Lu (1987) was employed. Configuration of the unit cell obtained by this way and hence the results of simulations vary from one run to another and, to be statistically meaningful, they should be averaged over a certain number of runs. The data given in the Table 6 were obtained by averaging over 30 realizations of QR structure: for all the numbers presented there, the standard deviation is well below 3%. It is well-known fact that $c_{\max}$ of the equal spheres random packing is about 0.63, close enough to the dense packing $c_{\max} = 0.68$ of BCC lattice. Comparison with the results obtained for the simple periodic structures (Tables 2 and 3) shows that the

Table 5
Effective anisotropy parameter, $(E_3^*/E_1^*)/A$

c	SC structure		BCC structure	
	$\lambda=0$	$\lambda=\infty$	$\lambda=0$	$\lambda=\infty$
0.1	0.957	0.957	0.933	0.957
0.2	0.939	0.933	0.855	0.928
0.3	0.925	0.923	0.829	0.901
0.4	0.913	0.924	0.766	0.869
0.5	0.900	0.933	0.707	0.831

Table 6
Effective elastic properties of a composite with QR lattice ($N = 16$) of cavities or rigid inclusions

c	C^*_{11}		C^*_{12}		C^*_{13}		C^*_{33}		C^*_{44}	
	$\lambda = 0$	$\lambda = \infty$	$\lambda = 0$	$\lambda = \infty$	$\lambda = 0$	$\lambda = \infty$	$\lambda = 0$	$\lambda = \infty$	$\lambda = 0$	$\lambda = \infty$
0.1	1.80	2.71	0.47	0.70	0.57	0.85	7.77	12.2	0.83	1.26
0.2	1.46	3.42	0.38	0.86	0.47	1.06	5.74	14.7	0.67	1.62
0.3	1.16	4.43	0.30	1.07	0.39	1.33	4.27	18.0	0.53	2.13
0.4	0.90	5.72	0.24	1.37	0.32	1.69	2.94	23.0	0.41	2.91
0.5	0.69	7.33	0.19	1.77	0.26	2.15	2.18	29.3	0.31	4.04

values obtained for a QR structure lie between the corresponding data for the simple cubic and BCC models and that BCC model is better approximation of disordered structure as compared with SC. Noteworthy, the anisotropy parameter $(C^*_{11} - C^*_{12})/2C^*_{66}$ calculated for QR model is close (within 2–3%) to 1. This result agrees well with the fact that a random structure composite of transversely isotropic matrix and rigid particles is transversely isotropic on macro level and we can consider it as another validation of our model.

The normalized values of C^*_{33} for three arrangement types considered by us are shown in Fig. 1. The dotted vertical lines represent $c_{\max}$ for each structure type (remind, $c_{\max}$ is equal to 0.52, 0.63 and 0.68 for SC, QR and BCC structure, respectively) and are, at the same time, asymptotic lines for C^*_{33} as $c \to c_{\max}$. When the particles are nearly in contact with their neighbours, convergence rate of the series (23)–(25) is rather slow and the number of harmonics one has to take into account to provide an accurate solution is prohibitively large. This extreme case requires a separate consideration: in the isotropic case $A = 1$, the asymptotic formulae for C^*_{ij} at $c \to c_{\max}$ have been derived by Nunan and Keller (1984). An asymptotic analysis of the problem is rather a subject of separate paper. However, our numerical study shows that the value C^*_{33}/C^-_{33} for a composite filled with rigid particles depends on A only marginally and it is believed that

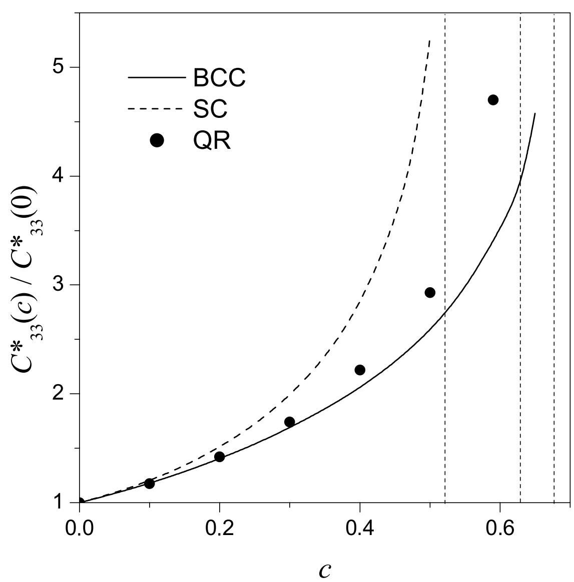

Fig. 1. Normalized modulus C^*_{33}/C^-_{33} as a function of disperse phase volume content, c.

the asymptotic analysis by Nunan and Keller (1984) with minor modifications can be applied to a composite with transversely isotropic matrix.

In the above numerical analysis, the inclusions were assumed very hard or very soft as compared with the matrix. In both cases, effect of inclusion orientation on the effective elastic response of composite is negligibly small. In fact, the interface conditions (2) reduce to $\mathbf{T}(\mathbf{u}^-)|_S = 0$ for $\lambda = 0$ and $\mathbf{u}^-|_S = 0$ for $\lambda = \infty$, effectively excluding inclusions from consideration. At finite λ, however, orientation of inclusions can influence the effective stiffness quite significantly. To estimate effect of orientation factor separately, we consider a composite with $\lambda = 1$: i.e., the inclusions are made from the same material as matrix does, $\mathbf{C}^+ = \mathbf{C}^-$. It can be thought, in particular, as a model of polycrystalline material with anisotropic grains. For the anisotropy axes of matrix and inclusions aligned, we have a homogeneous material with no local stress concentration and, hence, $\mathbf{C}^* = \mathbf{C}^-$ regardless on the volume fraction and arrangement type of particles. At the same time, misalignment of the phase materials results in considerable interface stress concentration (Kushch, 2003) and we can expect the effective moduli to be affected by rotation as well.

So, consider a periodic composite with simple (SC or BCC) lattice of inclusions ($\lambda = 1$) and restrict rotation of inclusions to the *xz*-plane. In this case, their orientation is determined uniquely by the single Euler's parameter β being an angle between the O_{z^-} and O_{z^+} axes. In Fig. 2, the normalized modulus C^*_{11}/C^-_{11} is given as a function of rotation angle β. Here, the solid lines represent C^*_{11} of composite with BCC structure with volume fraction of inclusions equal to 0.1, 0.3 and 0.5, respectively. The analogous data for a composite of SC symmetry are shown by the dashed lines. The matrix material considered is stiffer in *z*-direction ($E^-_3 = 5E^-_1$) and, expectably, C^*_{11} is growing with β increased and reaches at $\beta = \pi/2$ the maximum value which, in turn, grows monotonically with c. For non-dilute concentrations ($c \gtrsim 0.1$), the particles arrangement type also affects the stiffness of composite: so, at $c = 0.5 C^*_{11}$ is equal to 1.63 for SC and 1.93 for BCC lattice case. The corresponding data for the normalized modulus C^*_{33}/C^-_{33} are given in Fig. 3. Unlike C^*_{11}, C^*_{33} is reducing up to two times as β varies from 0 to $\pi/2$ whereas stiffness C^*_{22} in the direction of rotation axis remains practically unchanged.

The last example we consider is a periodic composite with the unit cell containing $N = 16$ arbitrarily oriented inclusions whose centers form a BCC lattice. On each run, the random number generator was

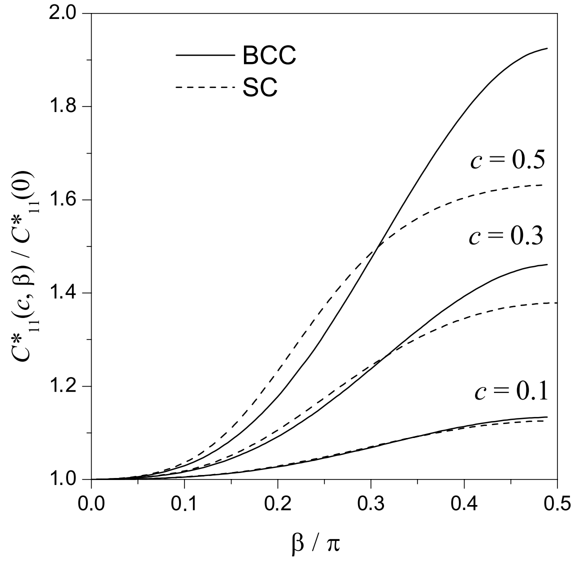

Fig. 2. Normalized modulus C^*_{11}/C^-_{11} as a function of rotation angle β.

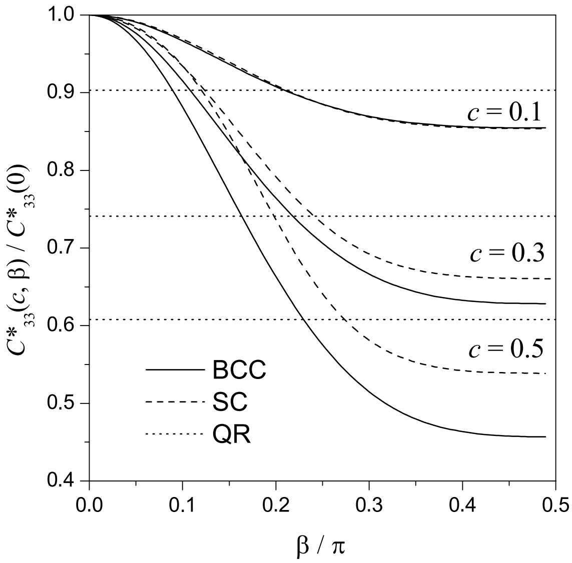

Fig. 3. Normalized modulus C^*_{33}/C^-_{33} as a function of rotation angle β.

Table 7
Effective elastic properties of a composite with BCC lattice ($N = 16$) of randomly oriented elastic inclusions, $\lambda = 1$

c	C^*_{11}	C^*_{12}	C^*_{13}	C^*_{33}	C^*_{44}
0.1	2.219	0.589	0.694	9.344	1.011
0.2	2.261	0.601	0.701	8.467	1.023
0.3	2.304	0.613	0.708	7.665	1.035
0.4	2.348	0.626	0.715	6.935	1.048
0.5	2.393	0.639	0.724	6.290	1.060
0.6	2.440	0.653	0.735	5.730	1.074

utilized to prescribe orientation of each separate particle and, for c given, averaging over 30 structure realizations was made to get the statistically valid data. The obtained by this way effective moduli are given in Table 7. Interestingly, these data are found to be practically invariant to the spatial arrangement of particles: simulations carried out for a unit cell with randomly placed and oriented inclusions gave the same, within 2–3%, results. This is correct, however, in the case $\lambda = 1$ only. For a general type disordered composite, both the arrangement and orientation statistics are to be taken into account.

6. Conclusions

The accurate and efficient analytical method has been developed to study the effective elastic properties of a matrix type particulate composite with transversely isotropic phases. The microgeometry of composite is modeled by a periodic structure with a unit cell containing a certain number of arbitrarily placed and oriented spherical inclusions. The analytical, multipole series expansion method of solution has been developed reducing the complicated primary periodic boundary-value problem for 3D multiple-connected domain to an ordinary set of linear algebraic equations and providing, thus, its high numerical efficiency. By analytical averaging the strain and stress fields, the exact formulae for the effective stiffness tensor have been derived. The numerical results given show an accuracy of the method and disclose the way and extent to which the selected structural parameters influence the macroscopic stiffness of composite.

Combination of the structural model flexible enough to approach an actual microstructure of composite with the fast numerical algorithm makes the method developed to be an efficient tool for reliable predicting the elastic properties of particulate composite with transversely isotropic phases. Although in the paper the inclusions were assumed to be spherical, the method with minor modifications (Kushch, 1997a) can be applied as well to study the effect of phase anisotropy in the composites with ellipsoidal inclusions and penny-shaped cracks.

Appendix A. Partial solutions of the equilibrium equations of transversely isotropic elastic solid

The complete sets of partial vectorial solutions of the equilibrium equations of transversely isotropic elastic solid have been introduced by Kushch (2004) using the well known representation of a general solution by means of three potential functions

$$u_x = \frac{\partial \Phi_1}{\partial x} + \frac{\partial \Phi_2}{\partial x} + \frac{\partial \Phi_3}{\partial y}, \quad u_y = \frac{\partial \Phi_1}{\partial y} + \frac{\partial \Phi_2}{\partial y} - \frac{\partial \Phi_3}{\partial x}, \quad u_z = k_1 \frac{\partial \Phi_1}{\partial z} + k_2 \frac{\partial \Phi_2}{\partial z}. \tag{A.1}$$

The functions Φ_j satisfy the quasi-harmonic equation

$$\left(\frac{\partial^2}{\partial x^2} + \frac{\partial^2}{\partial y^2} + v_j \frac{\partial^2}{\partial z^2} \right) \Phi_j = 0, \quad j = 1, 2, 3, \tag{A.2}$$

where $v_3 = 2C_{44}/(C_{11} - C_{12})$ whereas v_1 and v_2 are roots of the equation

$$C_{11} C_{44} v^2 - [(C_{44})^2 - C_{11} C_{33} - (C_{13} + C_{44})^2] v + C_{33} C_{44} = 0. \tag{A.3}$$

In (A.1), k_1 and k_2 are given by the expressions

$$k_j = \frac{C_{11} v_j - C_{44}}{C_{13} + C_{44}} = \frac{v_j (C_{13} + C_{44})}{C_{33} - v_j C_{44}}, \quad j = 1, 2. \tag{A.4}$$

In the case $v_1 \neq v_2$, representation (A.1) is general.

We introduce new spatial coordinates $x_j = x$, $y_j = y$, $z_j = z/\sqrt{v_j}$ to rewrite (A.2) as

$$\left(\frac{\partial^2}{\partial x_j^2} + \frac{\partial^2}{\partial y_j^2} + \frac{\partial^2}{\partial z_j^2} \right) \Phi_j = 0. \tag{A.5}$$

The sets of singular and regular solutions are given by (A.1), with the potential functions

$$\begin{aligned} \Phi_{ts}^{(j)} &= \frac{1}{(2t+1)} \left[F_{t+1}^{s}(\mathbf{r}_j, d_j) - F_{t-1}^{s}(\mathbf{r}_j, d_j) \right], \\ \phi_{ts}^{(j)} &= \frac{1}{(2t+1)} \left[f_{t+1}^{s}(\mathbf{r}_j, d_j) + f_{t-1}^{s}(\mathbf{r}_j, d_j) \right], \quad t = 0, 1, 2, \ldots; \ |s| \leqslant t+1, \end{aligned} \tag{A.6}$$

where

$$\begin{aligned} F_t^s(\mathbf{r}, d) &= \frac{(t-s)!}{(t+s)!} Q_t^s(\xi) P_t^s(\eta) \exp(\mathrm{i} s \varphi), \\ f_t^s(\mathbf{r}, d) &= \frac{(t-s)!}{(t+s)!} P_t^s(\xi) P_t^s(\eta) \exp(\mathrm{i} s \varphi) \end{aligned} \tag{A.7}$$

are the singular and regular, respectively, harmonic functions obtained by separation of variables in the Laplace equation written in the spheroidal coordinates (Hobson, 1931), P_t^s and Q_t^s are the associated Legendre functions of the first and second kind, respectively. In (A.6), $(\xi_j, \eta_j, \varphi_j)$ are given for $v_j < 1$ by the modified prolate spheroidal coordinates

$$\begin{aligned} &x + \mathrm{i}y = d_j \bar{\xi}_j \bar{\eta}_j \exp(\mathrm{i}\varphi_j), \qquad z = \sqrt{v_j} z_j = \sqrt{v_j} d_j \xi_j \eta_j, \\ &\bar{\xi}_j = \sqrt{(\xi_j)^2 - 1}, \qquad \bar{\eta}_j = \sqrt{1 - (\eta_j)^2}. \end{aligned} \tag{A.8}$$

In the case $v_j > 1$, one has to use the oblate spheroidal coordinates instead of prolate ones.

Note that, according to Hobson (1931), $F_t^s = f_t^s \equiv 0$ for $|s| > t$; this condition, however, makes it impossible to represent some of the singular solutions in the form (A.1) and (A.6). To resolve for this difficulty, we exploit the Podil'chuk's (1984) idea and introduced the following, additional to (A.7), functions of the form

$$F_t^{t+k}(\mathbf{r}, d) = \frac{1}{(2t+k)!} Q_t^{t+k}(\xi) P_t^{t+k}(\eta) \exp[\mathrm{i}(t+k)\varphi], \quad k = 1, 2, \ldots, \tag{A.9}$$

where

$$P_t^{t+k}(p) = \frac{(2t+k)!}{(1-p^2)^{(t+k)/2}} \underbrace{\int_p^1 \int_p^1 \cdots \int_p^1}_{t+k} P_t(p)(\mathrm{d}p)^{t+k} = \frac{(2t+k)!}{(1-p^2)^{(t+k)/2}} I_{t+k}$$

for $0 \leqslant p \leqslant 1$; for $p < 0$, $P_t^{t+k}(p) = (-1)^k P_t^{t+k}(-p)$. For the explicit expressions of I_{t+k}, see Kushch (2004). It is fairly straightforward to show that the functions (A.9) are the singular solutions of the Laplace equations but, unlike (A.7), they are discontinuous at $z = 0$. In the general series solution, however, these breaks cancel each other and give the continuous and differentiable expressions of the displacement and stress fields.

In (A.6), parameters of the modified spheroidal coordinate system (A.8) are chosen in a way that $\xi_j = \xi_{j0} = \text{const}$ at the surface $r = R$; i.e., S is the ξ-coordinate surface in each coordinate system introduced by (A.8). We provide this by defining

$$d_j = R/\xi_{j0}, \qquad \xi_{j0} = \sqrt{v_j/|v_j - 1|}.$$

In this case, moreover, we have $\eta_j = \theta$ and $\varphi_j = \varphi$ for $r = R$, where (r, θ, φ) are the ordinary spherical coordinates corresponding to the Cartesian ones (x, y, z). This is the key point: no matter how complicated is solution in the bulk, at the interface we get the linear combination of regular spherical harmonics $Y_t^s(\theta, \varphi) = P_t^s(\cos\theta)\exp(\mathrm{i}s\varphi)$. Under this circumstance, satisfaction the contact conditions at interface is the nothing more than standard algebra. To get the explicit expressions of the vectorial functions introduced, we substitute $\Phi_{ts}^{(j)}$ (A.6) into (A.1) and utilize the properties of the functions (A.7)

$$\begin{aligned} &\frac{d}{(2t+1)} \left(\frac{\partial}{\partial x} - \mathrm{i}\frac{\partial}{\partial y} \right) \left[F_{t+1}^s(\mathbf{r}, d) + F_{t-1}^s(\mathbf{r}, d) \right] = F_t^{s-1}(\mathbf{r}, d), \\ &\frac{d}{(2t+1)} \left(\frac{\partial}{\partial x} + \mathrm{i}\frac{\partial}{\partial y} \right) \left[F_{t+1}^s(\mathbf{r}, d) + F_{t-1}^s(\mathbf{r}, d) \right] = -F_t^{s+1}(\mathbf{r}, d), \\ &\frac{d}{(2t+1)} \frac{\partial}{\partial z} \left[F_{t+1}^s(\mathbf{r}, d) + F_{t-1}^s(\mathbf{r}, d) \right] = F_t^s(\mathbf{r}, d). \end{aligned} \tag{A.10}$$

It gives us the following set of singular vectorial solutions:

$$\begin{aligned}\mathbf{F}_{ts}^{(j)}(\mathbf{r}) &= F_t^{s-1}(\mathbf{r}_j, d_j)\mathbf{e}_1 - F_t^{s+1}(\mathbf{r}_j, d_j)\mathbf{e}_2 + \frac{k_j}{\sqrt{v_j}} F_t^s(\mathbf{r}_j, d_j)\mathbf{e}_3, \quad j = 1, 2, \\ \mathbf{F}_{ts}^{(3)}(\mathbf{r}) &= F_t^{s-1}(\mathbf{r}_3, d_3)\mathbf{e}_1 + F_t^{s+1}(\mathbf{r}_3, d_3)\mathbf{e}_2, \quad t = 0, 1, 2, \ldots, \quad |s| \leqslant t+1,\end{aligned} \tag{A.11}$$

where the complex Cartesian basis vectors are $\mathbf{e}_1 = (\mathbf{e}_x + \mathrm{i}\mathbf{e}_y)/2, \mathbf{e}_2 = (\mathbf{e}_x - \mathrm{i}\mathbf{e}_y)/2$ and $\mathbf{e}_3 = \mathbf{e}_z$.

At the spherical surface $r = R$, the functions $\mathbf{F}_{ts}^{(j)}(\mathbf{r})$ take the form

$$\begin{aligned}\mathbf{F}_{ts}^{(j)}(\mathbf{r})|_S &= Q_t^{s-1}(\xi_{j0})\chi_t^{s-1}\mathbf{e}_1 - Q_t^{s+1}(\xi_{j0})\chi_t^{s+1}\mathbf{e}_2 + \frac{k_j}{\sqrt{v_j}} Q_t^s(\xi_{j0})\chi_t^s\mathbf{e}_3, \quad j = 1, 2, \\ \mathbf{F}_{ts}^{(3)}(\mathbf{r})|_S &= Q_t^{s-1}(\xi_{30})\chi_t^{s-1}\mathbf{e}_1 + Q_t^{s+1}(\xi_{30})\chi_t^{s+1}\mathbf{e}_2, \quad t = 0, 1, 2, \ldots, \quad |s| \leqslant t+1,\end{aligned} \tag{A.12}$$

where $\chi_t^s = \frac{(t-s)!}{(t+s)!} Y_t^s(\theta, \varphi)$; the representation (A.12) is suitable for satisfying the interfacial boundary conditions (2) for displacements.

To satisfy the stress boundary conditions, we need similar expression of the traction vector $\mathbf{T_n} = \boldsymbol{\sigma} \cdot \mathbf{n}$. After somewhat involved algebra, we obtain the following representation of $\mathbf{T_n}(\mathbf{F}_{ts}^{(j)})$ at the surface S:

$$\begin{aligned}\frac{d_j}{C_{44}} \mathbf{T_n}(\mathbf{F}_{ts}^{(j)})|_S = &\frac{1}{\sqrt{v_j}} \left[(k_1 + 1) Q_t'^{s-1}(\xi_{j0}) - \frac{(s-1)}{\xi_{j0}} \frac{v_j C_{12} - k_j C_{13}}{v_j C_{44}} Q_t^{s-1}(\xi_{j0}) \right] \chi_t^{s-1}\mathbf{e}_1 \\ &- \frac{1}{\sqrt{v_j}} \left[(k_1 + 1) Q_t'^{s+1}(\xi_{j0}) + \frac{(s+1)}{\xi_{j0}} \frac{v_j C_{12} - k_j C_{13}}{v_j C_{44}} Q_t^{s+1}(\xi_{j0}) \right] \chi_t^{s+1}\mathbf{e}_2 \\ &+ (k_1 + 1) Q_t'^s(\xi_{j0})\chi_t^s\mathbf{e}_3, \quad j = 1, 2,\end{aligned} \tag{A.13}$$

$$\begin{aligned}\frac{d_3}{C_{44}} \mathbf{T_n}(\mathbf{F}_{ts}^{(3)})|_S = &\frac{1}{\sqrt{v_3}} \left[Q_t'^{s-1}(\xi_{30}) + (s-1) \frac{\xi_{30}}{(\bar{\xi}_{30})^2} Q_t^{s-1}(\xi_{30}) \right] \chi_t^{s-1}\mathbf{e}_1 \\ &+ \frac{1}{\sqrt{v_3}} \left[Q_t'^{s+1}(\xi_{30}) - (s+1) \frac{\xi_{30}}{(\bar{\xi}_{30})^2} Q_t^{s+1}(\boldsymbol{\xi}_{30}) \right] \chi_t^{s+1}\mathbf{e}_2 + \frac{1}{\sqrt{v_3}} \frac{s}{\bar{\xi}_{30}} Q_t^s(\xi_{30})\chi_t^s\mathbf{e}_3.\end{aligned}$$

The results exposed above imply $v_1 \neq v_2$. When $v_1 = v_2$, solution (A.1) is not general because of $\mathbf{F}_{ts}^{(1)} \equiv \mathbf{F}_{ts}^{(2)}$. In this case, however, the general solution of $\nabla \cdot \boldsymbol{\sigma} = 0$ can be represented as

$$u_x = \frac{\partial \Phi_1}{\partial x} + z\frac{\partial \Psi}{\partial x} + \frac{\partial \Phi_3}{\partial y}, \qquad u_y = \frac{\partial \Phi_1}{\partial y} + z\frac{\partial \Psi}{\partial y} - \frac{\partial \Phi_3}{\partial x}, \qquad u_z = \frac{\partial \Phi_1}{\partial z} + z\frac{\partial \Psi}{\partial z} - \frac{C_{13} + 3C_{44}}{C_{13} + C_{44}}\Psi \tag{A.14}$$

or, in the vectorial form,

$$\mathbf{u} = \nabla \Phi_1 + \nabla \times (\Phi_3 \mathbf{e}_z) + \left(z\nabla - \frac{C_{13} + 3C_{44}}{C_{13} + C_{44}} \mathbf{e}_z \right) \Psi, \tag{A.15}$$

where the potential function Ψ satisfies Eq. (A.2) with $v = v_1$. To get the complete set of independent solutions (A.11), one can take $\mathbf{F}_{ts}^{(2)}$ in the form

$$\mathbf{F}_{ts}^{(2)}(\mathbf{r}) = d_1 \left(z\nabla - \frac{C_{13} + 3C_{44}}{C_{13} + C_{44}} \mathbf{e}_z \right) F_t^s(\mathbf{r}_1, d_1) + \sqrt{v_1} d_1 (\xi_{10})^2 \nabla F_{t-1}^s(\mathbf{r}_1, d_1). \tag{A.16}$$

With the last term added, expression of $\mathbf{F}_{ts}^{(2)}$ at the surface $r = R$ is rather simple:

$$\begin{aligned}\mathbf{F}_{ts}^{(2)}(\mathbf{r})|_S = &\sqrt{v_1} \frac{\xi_{10}}{(t+s)} Q_{t-1}^{s-1}(\xi_{10})\chi_t^{s-1}\mathbf{e}_1 - \sqrt{v_1} \frac{\xi_{10}}{(t+s+2)} Q_{t-1}^{s+1}(\xi_{10})\chi_t^{s+1}\mathbf{e}_2 \\ &+ \left[\frac{\xi_{10}}{(t+s+1)} Q_{t-1}^s(\xi_{10}) - \frac{C_{13} + 3C_{44}}{C_{13} + C_{44}} Q_t^s(\xi_{10}) \right] \chi_t^s\mathbf{e}_3.\end{aligned} \tag{A.17}$$

For the expression of the corresponding traction vector, see Podil'chuk (1984).

The explicit form of the regular solutions $\mathbf{f}_{ts}^{(j)}$ is given by Eq. (A.11) with the replace F_t^s to f_t^s. To get the expression of $\mathbf{f}_{ts}^{(j)}$ and $\mathbf{T}_\mathbf{n}(\mathbf{f}_{ts}^{(j)})$ at the interface, one has to substitute $Q_t^s(\xi)$ by $P_t^s(\xi)$ in (A.12) and (A.13), respectively.

Appendix B. Evaluation of the triple lattice sums

The triply periodic solutions $\widehat{F}_{ts}$ of the Laplace equation entering the expression of $\mathbf{F}_{ts}^{(j)}$ are

$$\widehat{F}_{ts}(\mathbf{r}, d) = \sum_{\mathbf{k}} F_t^s(\mathbf{r} + \mathbf{R}_\mathbf{k}, d), \tag{B.1}$$

where $\mathbf{R}_\mathbf{k} = a(k_1\mathbf{e}_x + k_2\mathbf{e}_y + k_3\mathbf{e}_z)$, a being the cubic lattice period, and summation is made over all the integer k_1, k_2 and k_3. Theory and application of the functions (B.1) for $|s| \leqslant t$ is given elsewhere (Kushch, 1997a); below, we outline briefly an idea of the summation technique and give the necessary formulae.

Obtaining the local expansion of the periodic functions $\widehat{F}_{ts}$ is based on the re-expansion formulae for the singular solid spheroidal harmonics F_t^s (Kushch, 1997a) written in our case $d_1 = d_2 = d$ as

$$F_t^s(\mathbf{r} + \mathbf{R}, d) = \sum_{k=0}^{\infty} \sum_{|l| \leqslant k} \eta_{tk}^{(s-l)}(\mathbf{R}, d) f_k^l(\mathbf{r}, d), \tag{B.2}$$

where the general expression of η_{tk}^s is

$$\eta_{tk}^s(\mathbf{R}, d) = \eta_{tks}^{(1)} = (-1)^{k+s} \sum_{r=0}^{\infty} N_{tkr}(d) F_{t+k+2r}^s(\mathbf{R}, 2d), \tag{B.3}$$

$$N_{tkr} = \sqrt{\pi}(k + 1/2) d^{2r+t+k+1}(t + k + 2r + 1/2) \times \sum_{j=0}^{r} \frac{(-1)^j}{(r-j)!} \left(\frac{1}{2}\right)^{2j+t+k+1} \Gamma(t + k + r + j + 1/2) M_{tkj} \tag{B.4}$$

and

$$M_{tkj} = \frac{(t + k + j + 2)_j}{j!\Gamma(t + j + 3/2)\Gamma(k + j + 3/2)}. \tag{B.5}$$

Here, $\Gamma(z)$ is the Gamma-function and $(n)_m$ is the Pochhammer's symbol.

In the case of well-separated inclusions, namely for $\|\mathbf{R}\| > 2d$, expression of η_{tk}^s can be simplified to

$$\eta_{tk}^s(\mathbf{R}, d) = \eta_{tks}^{(2)} = (-1)^{k+s} \sum_{r=0}^{\infty} L_{tkr}(d) S_{t+k+2r}^s(\mathbf{R}), \tag{B.6}$$

where the functions

$$S_t^s(\mathbf{r}) = \frac{(t-s)!}{r^{t+1}} Y_t^s(\theta, \varphi), \quad \text{and} \quad s_t^s(\mathbf{r}) = \frac{r^t}{(t+s)!} Y_t^s(\theta, \varphi) \tag{B.7}$$

are the singular and regular, respectively, solid spherical harmonics and

$$L_{tkr} = \pi(k + 1/2)(d/2)^{2r+t+k+1} M_{tkr}. \tag{B.8}$$

In practice, this simplified formula provides an efficient calculation of η_{tk}^s for $\|\mathbf{R}\| \gtrsim 2.5d$, where the convergence rate of the series (B.6) becomes sufficiently high. Noteworthy, all the above formulae remain valid for the extended set of spheroidal harmonics given by (A.9) provided we define

$$S_t^{t+k}(\mathbf{r}) = \frac{1}{r^{t+1}} P_t^{t+k}(\cos\theta)\exp[\mathrm{i}(t+k)\varphi]. \tag{B.9}$$

Now, we apply (B.2) to all the terms of the sum (B.1) but one with $\mathbf{k} = 0$ to obtain, after change of summation order, a local expansion of $\widehat{F}_{ts}$ in the vicinity of the point $\mathbf{R} = 0$:

$$\widehat{F}_{ts}(\mathbf{r}, d) = F_t^s(\mathbf{r}, d) + \sum_{k=0}^{\infty} \sum_{|l| \leqslant k} \hat{\eta}_{tk,s-l}(0, d) f_k^l(\mathbf{r}, d), \tag{B.10}$$

where the expansion coefficients are the triple infinite (lattice) sums

$$\hat{\eta}_{kts}(\mathbf{R}, d) = \sum_{\mathbf{k}\neq 0} \eta_{kt}^s(\mathbf{R} + \mathbf{R_k}, d). \tag{B.11}$$

In the vicinity of the point $\mathbf{r} = \mathbf{R} \neq 0$, the local expansion takes the form

$$\widehat{F}_{ts}(\mathbf{r}, d) = \sum_{k=0}^{\infty} \sum_{|l| \leqslant k} \widehat{\eta}_{tk,s-l}(\mathbf{R}, d) f_k^l(\mathbf{r}, d), \tag{B.12}$$

in this case, the term with $\mathbf{k} = 0$ is present in the sum (B.11) as well.

Evaluation of the sums (B.11) is the most difficult and time-consuming part of numerical algorithm. We make use advantage of possessing two representations of η_{tk}^s to rewrite it in a suitable for computational purpose form:

$$\hat{\eta}_{tks}(\mathbf{R}, d) = \sum_{\|\mathbf{r}+\mathbf{R_k}\| \leqslant 2.5d} \left[\eta_{tks}^{(1)}(\mathbf{R} + \mathbf{R_k}, d) - \eta_{tks}^{(2)}(\mathbf{R} + \mathbf{R_k}, d)\right] + \hat{\eta}_{tks}^{(2)}(\mathbf{R}, d), \tag{B.13}$$

where

$$\hat{\eta}_{tks}^{(2)}(\mathbf{R}, d) = \sum_{r=0}^{\infty} L_{tkr} \widehat{S}_{t+k+2r,s}(\mathbf{R}) \tag{B.14}$$

and

$$\widehat{S}_{ts}(\mathbf{R}) = \sum_{\mathbf{k}} S_t^s(\mathbf{R} + \mathbf{R_k}). \tag{B.15}$$

The first term in (B.13) is a finite sum and, thus, the only remaining problem is evaluation of the lattice sums $\widehat{S}_{ts}$. For $|s| \leqslant t$, the efficient algorithms of fast summation are well developed now (e.g. Zinchenko, 1994). An attempt to extend the Evald's summation technique on the spherical harmonics with $|s| > t$ meets, however, certain mathematical difficulties. Therefore, we shall apply here an alternate method of summation based on using of double Fourier series. This method, used systematically by Golovchan et al. (1993), is somewhat more involved but provides rather simple and efficient numerical realization. What is important here, it works equally well for the sums (B.15) with $|s| > t$.

The summation technique is briefly shown below where we put, for simplicity sake, $\mathbf{R} = 0$. Taking into account that $\widehat{S}_{ts}$ are absolutely convergent for $t \geqslant 2$, we decompose them into a sum of two parts:

$$\widehat{S}_{ts}(\mathbf{0}) = \widehat{S}_{ts}^{(1)}(\mathbf{0}) + \widehat{S}_{ts}^{(2)}(\mathbf{0}) = \left(\sum_{\substack{k_1,k_2 \\ (k_3=0)}} + \sum_{\substack{\mathbf{k} \\ (k_3\neq 0)}} \right) S_t^s(\mathbf{R_k}). \tag{B.16}$$

The first term $\widehat{S}_{ts}^{(1)}$ is a double series: to evaluate it, either the direct summation or, for the lower values of t, the fast summation technique described by Golovchan et al. (1993) can be applied. To find $\widehat{S}_{ts}^{(2)}$, we rewrite it as

$$\widehat{S}_{ts}^{(2)}(\mathbf{0}) = \sum_{k_3 \neq 0} \widehat{S}_{ts}^{(1)}(ak_3\mathbf{e}_z). \tag{B.17}$$

In the half-spaces $z \lessgtr 0$, $\widehat{S}_{ts}^{(1)}$ is the regular double-periodic function and, thus, allows representation by the double Fourier series

$$\widehat{S}_{ts}^{(1)}(\mathbf{r}) = \sum_{m,n} (-1)^{t+s} \zeta_{mn}^{ts} \exp[-\delta_{mn}|z| + \mathrm{i}(\alpha_m x + \alpha_n y)], \quad z \lessgtr 0, \tag{B.18}$$

where

$$\alpha_m = \frac{2\pi m}{a}, (\delta_{mn})^2 = (\alpha_m)^2 + (\alpha_n)^2 \quad \text{and} \quad \zeta_{mn}^{ts} = \frac{2\pi}{a^2}(\delta_{mn})^{t-s-1}(\alpha_n - \mathrm{i}\alpha_m)^s. \tag{B.19}$$

By combining (B.17) and (B.18) one obtains, after some algebra, the rapidly convergent series

$$\widehat{S}_{ts}^{(2)}(\mathbf{0}) = [1 + (-1)^{t+s}] \sum_{m,n} \zeta_{mn}^{ts} [\exp(\delta_{mn} a) - 1]^{-1}. \tag{B.20}$$

The formulae (B.16)–(B.20) are valid for $|s| \leqslant t + 2$ and thus can be used alone or as a supplement to the Evald's technique to evaluate the sums (B.15) and thus $\hat{\eta}_{kts}$ (B.11), entering the matrix of the resolving set of Eqs. (29).

References

Bateman, G., Erdelyi, A., 1953. Higher Transcendental Functions, vol. 2. McGraw Hill, New York.

Golovchan, V.T., Guz, A.N., Kohanenko, Yu., Kushch, V.I., 1993. Mechanics of Composites (in 12 volumes). In: Statics of Materials, vol. 1. Naukova dumka, Ukraine.

Fraysse, V., Giraud, L., Gratton, S., 1998. A set of GMRES routines for real and complex arithmetics. CERFACS Technical Report TR/PA/97/49.

Hobson, E.W., 1931. The Theory of the Spherical and Ellipsoidal Functions. Cambridge University Press.

Iwakuma, T., Nemat-Nasser, S., 1983. Composites with periodic microstructure. Computers and Structures 16, 13–19.

Kanaun, S.K., Levin, V.M., 1994. The self-consistent field method in mechanics of matrix composite materials, in: Marker, K.Z. (Ed.), Advances in Mathematical Modelling of Composite Materials. World Scientific Publication, Singapore.

Khoroshun, L.P., Maslov, B.P., Leshchenko, P.V., 1989. Prediction the Effective Properties of Piezoactive Composite Materials. Naukova dumka, Ukraine.

Kushch, V.I., 1987. Computation of the effective elastic moduli of a granular composite material of regular structure. Soviet Applied Mechanics 23, 362–365.

Kushch, V.I., 1997a. Conductivity of a periodic particle composite with transversely isotropic phases. Proceedings of the Royal Society of London A 453, 65–76.

Kushch, V.I., 1997b. Microstresses and effective elastic moduli of a solid reinforced by periodically distributed spheroidal inclusions. International Journal of Solids and Structures 34, 1353–1366.

Kushch, V.I., 2003. Stress concentration in the particulate composite with transversely isotropic phases. International Journal of Solids and Structures, in press.

Kushch, V.I., Sangani, A.S., 2000. Stress intensity factor and effective stiffness of a solid containing aligned penny-shaped cracks. International Journal of Solids and Structures 37, 6555–6570.

Mura, T., 1982. Micromechanics of Defects in Solids. Martinus Nijhoff, Netherlands.

Nemat-Nasser, S., Yu, N., Hori, M., 1993. Solids with periodically distributed cracks. International Journal of Solids and Structures 30, 2071–2095.

Nunan, C.K., Keller, J.B., 1984. Effective elasticity tensor of a periodic composite. Journal of the Mechanics and Physics of Solids 32, 259–280.

Podil'chuk, Yu.N., 1984. The Boundary Value Problems of Statics of Elastic Solid. Naukova Dumka, Ukraine.

Rodriguez-Ramos, R., Sabina, F.J., Guinovart-Diaz, R., Bravo-Castillero, J., 2001. Closed-form expressions for the effective coefficients of a fiber-reinforced composite with transversely isotropic constituents—I. Elastic and square symmetry. Mechanics of Materials 33, 223–235.

Sangani, A.S., Lu, W., 1987. Elastic coefficients of composites containing spherical inclusions in a periodic array. Journal of the Mechanics and Physics of Solids 35, 1–21.

Sangani, A.S., Mo, G., 1995. An O(N) algorithm for Stokes and Laplace interaction of particles. Physics of Fluids 8, 1990–2010.

Sangani, A.S., Mo, G., 1997. Elastic interactions in particulate composite with perfect as well as imperfect interfaces. Journal of the Mechanics and Physics of Solids 45, 2001–2031.

Sevostianov, I., Levin, V., Kachanov, M., 2001. On the modeling and design of piezocomposites with prescribed properties. Archives of Applied Mechanics 71, 733–747.

Sevostianov, I., Yilmaz, N., Kushch, V., Levin, V., 2003. Effective elastic properties of matrix composites with transversely isotropic phases. International Journal of Solids and Structures, submitted for publication.

Willis, J.R., 1975. The interactions of gas bubbles in an anisotropic elastic solid. Journal of the Mechanics and Physics of Solids 23, 129–138.

Willis, J.R., 1977. Bounds and self-consistent estimates for the overall properties of anisotropic composites. Journal of the Mechanics and Physics of Solids 25, 185–202.

Withers, P.J., 1989. The determination of the elastic field of an ellipsoidal inclusion in a transversely isotropic medium, and its relevance to composite materials. Philosophical Magazine 59, 759–781.

Zinchenko, A.Z., 1994. An efficient algorithm for calculating multiparticle interaction in a concentrated dispersion of spheres. Journal of Computational Physics 111, 120–135.